Synthesis, Kinetic Study and Molecular Orbital Investigation of Cadmium(II), Mercury(II) and Lead(II) Complexes with the Mixed Pendant-Arm Macrocyclic Ligand 1,7-Bis(carboxymethyl)-4,10-bis(1-methylimidazol-2-ylmethyl)-1,4,7,10-tetraazacyclododecane

Massimo Di Vaira,[a] Fabrizio Mani,[a] Stefano Seniori Costantini,[a] Piero Stoppioni,*[a] and Alberto Vacca[a]

Keywords: Macrocyclic ligands / Cadmium / Lead / Mercury / Conformational equilibrium / Density functional calculations

The neutral $[ML^6]\cdot 3H_2O$ complexes (M = Cd^{II}, Hg^{II} and Pb^{II}) formed with the potentially octadentate ligand 1,7-bis(carboxymethyl)-4,10-bis(1-methylimidazol-2-ylmethyl)-1,4,7,10-tetraazacyclododecane (H_2L^6) in its anionic deprotonated form, which bears two pairs of different dangling groups in *trans* positions on the cyclen skeleton, have been synthesized. Their low-temperature limiting NMR spectra (^1H and ^{13}C) in D_2O show that both the dangling groups and the ethylenic moieties of the macrocycle ring are in a fixed conformation in all complexes at 273 K. These conditions are relaxed at higher temperatures, yielding a dynamic behaviour that proceeds through both ring inversion and rearrangement of the pendant arms. The kinetic parameters for ring inversion have been obtained from the temperature-dependent ^{13}C NMR spectra. Cd: k(298 K) = 236 s^{-1}; $\Delta H^{\ddagger}$ = 72.9 ± 0.6 kJ·mol^{-1}; $\Delta S^{\ddagger}$ = 45 ± 2 J K^{-1}·mol^{-1}; Hg: k(298 K) = 292 s^{-1}; $\Delta H^{\ddagger}$ = 68 ± 3 kJ·mol^{-1}; $\Delta S^{\ddagger}$ = 29 ± 10 J K^{-1}·mol^{-1}; Pb: k(298 K) = 122 s^{-1}; $\Delta H^{\ddagger}$ = 65 ± 2 kJ·mol^{-1}; $\Delta S^{\ddagger}$ = 14 ± 5 J K^{-1}·mol^{-1}. In the absence of experimental structure determinations, some insight into the geometries has been obtained by quantum-mechanical calculations.

Introduction

Considerable attention has been addressed to metal complexes of 1,4,7,10-tetraazacyclododecane (cyclen) bearing pendant arms.[1−6] Depending on the number of substituent groups on the macrocyclic framework, as well as on the requirements of the metal ions employed, the substituted cyclen ligands easily adapt to coordination numbers six[7−9] seven[10] or eight,[11−13] and thus they might coordinate mono-, di- and trivalent metal ions. Complexes with these ligands exhibit notable thermodynamic stability and kinetic inertia and, consequently, they have important applications in, for example,[14] (i) the design of luminescent chelates for immunoassays,[6,15,16] (ii) use of Gd-containing contrast agents in diagnostic medicine[17,18] and (iii) labelling and specific cleavage of DNA and RNA.[19−21]

Representative examples of such ligands include the 1,4,7,10-tetraazacyclododecane-tetraacetic acid (H_4DOTA), which can provide anionic donors on the dangling groups, and molecules bearing four neutral donors on the arms of functionalized tetraazacyclododecane (Scheme 1).[7,22−26] Crystal data of the complexes have revealed that the four nitrogen atoms of the macrocycle and the four donors from the dangling groups are arranged in two parallel squares that are tilted by an angle denoted as α (Scheme 2). The coordination geometry can range from a regular antiprism (α = 45°) to a prism (α = 0°). Neither limiting case has been observed so far, and most known geometries cluster around two values: α = 40° and 15° (A and B, respectively, in Scheme 2).[7,26−32]

We have synthesized potentially octadentate ligands based on tetraazacyclododecane bearing, on the pendant arms, either four pyrazoles, L^5,[33] or two pairs of different groups in *trans* positions, namely two methylimidazoles and two carboxy groups, H_2L^6 [9] (Scheme 3). The solid manganese and cadmium complexes with L^5 have nearly prismatic structures,[34,35] a geometry that is preferred in solution by some lanthanide complexes with L^6.[36] Generally, the eight donors of the octadentate ligands L^1−L^6 are also considered to be bound to the metal ion in solution, a notable exception being the seven-coordinate magnesium complex with 1,4,7,10-tetrakis(2-methoxyethyl)-1,4,7,10-tetraazacyclododecane (L^4), which has the oxygen of a pendant arm uncoordinated.[10] Most of the complexes undergo dynamic behaviour in solution, which has been rationalized in terms of an exchange process between two enantiomers,[29,30] at

[a] Dipartimento di Chimica, Università di Firenze,
Via della Lastruccia 3, 50019 Sesto Fiorentino, Italy
E-mail: piero.stoppioni@unifi.it

Supporting information for this article is available on the WWW under http://www.eurjic.org or from the author.

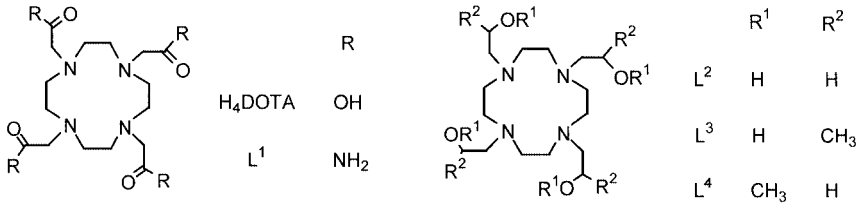

Scheme 1

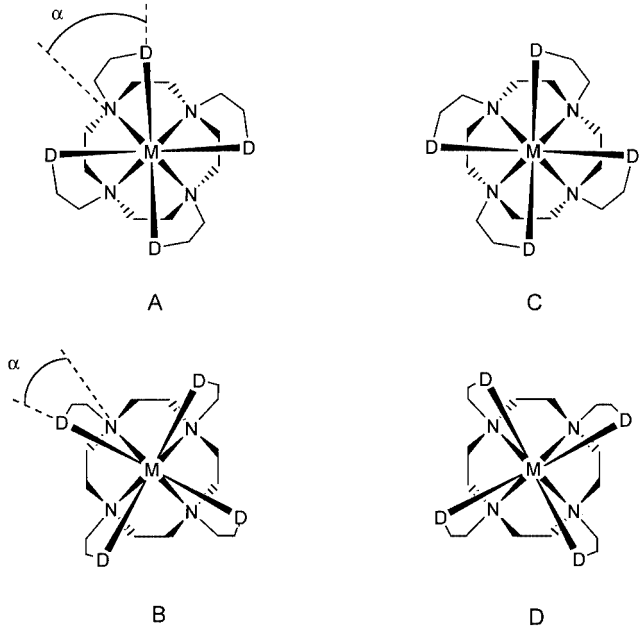

Scheme 2

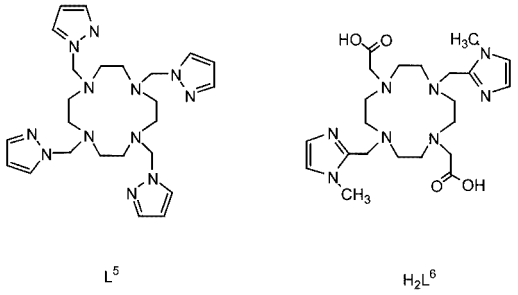

Scheme 3

rates within the ^{13}C NMR timescale. In this paper we report both on the synthesis of complexes formed by the "mixed" H_2L^6 ligand (Scheme 3) in the anionic form with different size metal ions (Cd^{II}, Hg^{II} and Pb^{II}) and on their dynamic behaviour in solution by using variable-temperature ^1H and ^{13}C NMR spectroscopy. As repeated attempts to obtain suitable crystals of the compounds for X-ray investigations failed, quantum mechanical calculations were undertaken to obtain information on their geometry and bonding.

Results and Discussion

Syntheses of the Metal Complexes

The cadmium derivative was prepared by direct reaction of cadmium carbonate with the ligand H_2L^6, dissolved in water. The mercury and lead derivatives were prepared in water by reacting the acetate of the metal with the ligand and then neutralizing the resulting solution with Na_2CO_3. The complexes obtained after workup crystallize with three water molecules, $[ML^6]\cdot 3H_2O$, and are very soluble in polar solvents (water, methanol and ethanol). As expected for such compounds, they are stable in solution for weeks in the pH range 5−10.[37]

NMR Spectra of the Complexes

The $^{13}C\{^1H\}$ spectrum of the cadmium complex at 273 K exhibits eleven peaks which, on the basis of data for lanthanide complexes with the same ligand, are assigned as δ = 177.7 ppm to the carboxylate functionalities, δ = 145.8, 125.6 and 122.5 ppm to the carbon atoms of the imidazole rings, δ = 57.4 and 48.4 ppm to the methylenic carbon atoms of the acetate and of the imidazole arms, respectively, δ = 51.8, 50.9, 48.4 and 48.1 ppm to the ethylenic carbons of the tetraazamacrocycle, and δ = 32.0 ppm to the methyl carbon of imidazole. The signals of two equivalent carbons of the macrocycle and of the two carbons of the imidazole CH_2 bridges have the same shift (δ = 48.4 ppm) and yield a resonance of comparatively higher intensity. The C^2 carbon of imidazole couples with the metal ($^2J^{13}_{C\text{-}}{}^{111}_{Cd}$ = 13.1 Hz), which does not change in the range of temperatures investigated. On increasing the temperature the four signals due to the macrocycle broaden, collapse, and then merge (Figure 1) to afford, at 358 K, two resonances at δ = 50.3 and 49.7 ppm; the signals due to the other carbon atoms remain narrow, undergoing small drifts. The proton NMR spectrum of the cadmium derivative shows thirteen resonances at 273 K (see the Exp. Sect.) which have been assigned with the aid of a 2D COSY experiment. The imidazole protons appear as a pair of doublets at low field and those of the methyl group yield a singlet at δ = 3.28 ppm. The protons of the CH_2COO^- moiety yield two doublets (δ = 3.69 and 3.34 ppm; J = 15 Hz). The CH_2 bridging the macrocycle and the imidazole yields a doublet (δ = 2.56 ppm; J = 16 Hz) and a resonance (δ = 2.28 ppm) which overlaps with those of the macrocycle. Such resonances, also seen, with minor changes, for diamagnetic lanthanide complexes with L^6,[36] are typical of two non-equivalent AB

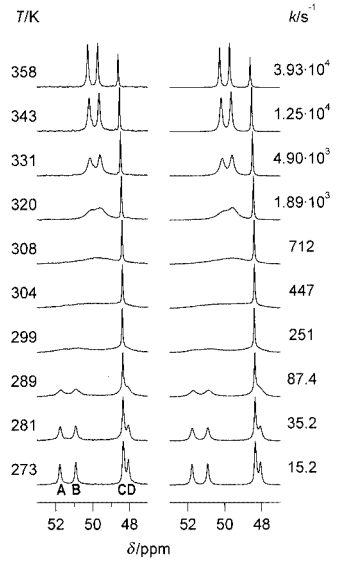

Figure 1. $^{13}C\{^1H\}$ spectra of the macrocyclic carbons of the [CdL^6] complex at different temperatures (left) compared with spectra calculated by line-shape analysis (right). The simulation has been performed by assuming an ABCD → CDAB exchange mechanism

systems.[38,39] The ethylenic moieties of the macrocycle present four triplets at δ = 3.01, 2.91, 2.67 and 2.37 ppm (coupling constants ca. 12.0 Hz), overlapping doublets centered at δ = 2.28 ppm and two doublets at δ = 2.05 and 1.86 ppm (coupling constant ca. 12.0 Hz). The chemical shifts of the resonances around δ = 2.7 and 2.1 ppm, and the multiplicity and coupling constants, are typical of two nonequivalent ABCD systems exhibiting large geminal and axial couplings, with small equatorial couplings. Such systems parallel those observed at low temperature for the ethylenic groups of lanthanum(III) and lutetium(III) complexes with L^6;[36] furthermore, each ABCD system is similar to that exhibited by diamagnetic lanthanide complexes with DOTA.[38,39] By increasing the temperature the three resonances due to the protons of methylimidazole remain narrow, undergoing a low-field shift; all the other resonances broaden, collapse, and then merge to afford a spectrum which exhibits, at 358 K, narrow signals at δ = 4.46 and 3.37 ppm for the CH_2 of the dangling groups and two unresolved resonances centered at δ = 3.54 and 3.25 ppm, due to the ethylenic moieties of the macrocycle.

The mercury and lead derivatives yield ^1H and ^{13}C NMR spectra at low temperature which parallel that of the cadmium complex; the shift of each signal is marginally affected by the nature of the metal (see the Exp. Sect.), which induces partial overlapping of some resonances so that they may appear as complex multiplets. The coupling constant between the C^2 imidazole carbon atom and mercury ($^2J^{13}_{C\text{-}^{199}Hg}$ = 54 Hz) does not change in the range of temperatures investigated. However, for no obvious reason, a similar coupling is not observed in the [PbL^6] spectrum (nor with the [PbL^1]$^+$ complex cation[7]), possibly due to either a low intensity or a small coupling constant for the ^{207}Pb satellites.[7] Both the ^{13}C and ^1H spectra of the mercury and lead complexes change with increasing temperature, as found for the cadmium derivative. At the highest temperature (Hg, 346 K, Pb 353 K) they exhibit two signals for the macrocycle (Hg, δ = 49.2 and 48.8 ppm; Pb, 49.8 and 49.7 ppm) in the ^{13}C spectra; in the proton spectra they exhibit narrow signals (Hg, δ = 4.37 and 3.27 ppm; Pb, δ = 4.50 and 3.70 ppm) for the CH_2 of the dangling groups and two unresolved resonances (Hg, δ = 3.45 and 3.20 ppm; Pb, δ = 3.55 and 3.45 ppm) due to the ethylenic moieties.

Similarities between the NMR spectroscopic data for the present cadmium, mercury and lead derivatives at the low exchange limit and the spectra of other metal complexes with L^5 and L^6, which either possess a nearly prismatic geometry in the solid state[34,35] or have been assigned that geometry in solution,[36] suggest that the same conformation should also be assigned to the present [ML^6] species. This view is supported by the quantum mechanical calculations (see below). Conversely, the variable temperature NMR experiments reveal that the conformational equilibria are thermally activated. Interconversion processes between the conformational isomers may occur via (a) simple rearrangement ("rotation") of the pendant arms (A → B or C → D, in Scheme 2), (b) macrocycle ring inversion (A → C or B → D) or (c) combinations of both types of motion,[40,53] which may afford interconversion between enantiomers. The coupling detected between the Cd or Hg atom and one imidazole carbon over the whole temperature range, which is consistent with previous results for lanthanide analogues,[36] suggests that the rearrangements occur without detachment of the pendant arms (but see below, computational results for Hg species). The above interconversion processes, particularly process (b), involve changes in the magnetic environment of the macrocycle carbon atoms, which may be characterized by a four-site line-shape analysis. Typical experimental and calculated ^{13}C NMR spectra for the cadmium complex are displayed in Figure 1. The temperature dependence of the rate constants, fitted according to the Eyring equation, yielded the parameters: Cd, k(298 K) = 236 s^{-1}, $\Delta H^{\ddagger}$ = 72.9 ± 0.6 kJ·mol^{-1}, $\Delta S^{\ddagger}$ = 45 ± 2 J^{-1}·mol^{-1}; Hg, k(298 K) = 292 s^{-1}, $\Delta H^{\ddagger}$ = 68 ± 3 kJ·mol^{-1}, $\Delta S^{\ddagger}$ = 29 ± 10 J K^{-1}·mol^{-1} and Pb, k(298 K) = 122 s^{-1}, $\Delta H^{\ddagger}$ = 65 ± 2 kJ·mol^{-1}, $\Delta S^{\ddagger}$ = 14 ± 5 J K^{-1}·mol^{-1} (details are given with the Supporting Information, see also the footnote on the first page article). The kinetic parameters for compounds with the L^1−L^4 or DOTA ligands are affected by the nature of the donor atoms on the dangling groups and by the metal, or the solvent,[7,10,41] and are higher for complexes with anionic donors on the arms. The kinetic parameters of the present [ML^6] compounds compare best with those of lanthanum complexes formed with DOTA[38] or L^6,[36] being significantly larger than those of compounds with four neutral donors on the arms. This may be due to the presence of two anionic donors on L^6 and, in part, to the nature of the metal atoms. Line shape analysis of the ^{13}C NMR peaks due to the macrocycle carbon atoms provides direct kinetic information on the macrocycle ring inversion, rather than on rotation of the arms. However, the ^1H NMR spectra show that both ring inversion and arm rotation occur sim-

ultaneously in the temperature range studied, as indicated by the loss of rigidity of all of the NCH_2CH_2N, NCH_2COO^- and NCH_2MeIz moieties with increasing temperature. The rate constants for the above processes (a) and (b) were not measured by ^1H NMR spectroscopic data due to the complexity of the exchanging system. However, as both processes occur in the same temperature range their rate constants should be similar, so that all types of interconversions may take place.

Quantum-Mechanical Calculations

For the [ML^6] systems considered here, calculations on gas-phase models yielded two low-energy conformers, with closely spaced energies ($\leq$ 13 kJ·mol^{-1} energy differences). Their geometries broadly correspond to the idealized coordination types of Scheme 2, but precisely defined geometrical parameters (detailed below) are needed for the following discussion. The upper/lower arrangements of Scheme 2 will be, respectively, denoted by *ap* and *iap*, for "*a*nti*p*rismatic" and "*i*nverted *a*nti*p*rismatic ", as previously used to describe the analogous coordination modes in the related DOTA systems.[40,53] The cadmium conformers will, accordingly, be denoted Cd*ap* and Cd*iap*, and so on. Optimized geometries for the two Cd conformers are shown in Figure 2, and selected geometrical parameters, as well as energy differences between the low-energy conformers of each metal system, are given in Table 1.

The two fundamental geometries may be identified unambiguously by the signs of the torsion angles of the ethylenic chains of the macrocycle, τ_1 and τ_2 in Table 1, and those of the dangling groups, τ_3 and τ_4. The signs are all negative for an "idealized *iap*" conformer, such as Cd*iap* in Figure 2 (they would be all positive for its enantiomer), whereas the signs are opposite in pairs, τ_1 and τ_2 with respect to τ_3 and τ_4, for a "pure *ap*" conformer, such as Cd*ap*. These sign distributions, however, do not match the present Pb and Hg models, due to inconsistent τ_4 signs (Table 1). Therefore, the *ap*/*iap* assignments for the latter systems were based solely on consideration of the τ_{1-3} signs. Indeed, unlike the present Cd and the previous lanthanide models,[53] the angle (β in Table 1) by which the plane of the imidazole group is bent away from the line connecting the metal and the heterocycle N donor (N_{im} hereafter; the macrocycle nitrogens are collectively labelled N_{mac}) is exceedingly large for the two lowest energy conformers of both the Pb and the Hg systems. The lowest energy, Pb*iap* and Hg*iap*, conformers are shown in Figure 3 and more representations are shown in the Supporting Information. These arrangements suggest weaker interactions between the Pb or Hg atom and the "neutral" dangling groups than those between the metal and the charged carboxylates. This is particularly evident for the Hg species, where the imidazole groups lie at considerable distances from the metal (Table 1). The difference under discussion between the Pb and the Cd (or the lanthanide[53]) models may be ascribed to the smaller charge/radius ratio of the former cation and to the strain imposed

Table 1. Values of selected geometrical parameters and energy differences between conformers for the [ML^6] model systems

Model system[a]	Cd*iap*	Cd*ap*	Pb*iap*	Pb*ap*	Hg*iap*	Hg*ap*
Relative energy[b]	0	9.29	0	12.29	0	13.43
M−N1	2.687	2.634	2.809	2.732	2.600	2.575
M−N2	2.737	2.798	2.775	2.884	2.687	2.770
M−O1	2.282	2.284	2.471	2.468	2.252	2.244
M−N4	2.485	2.460	2.959	2.924	3.788	3.491
τ_1[c]	−59.1	−56.5	−58.0	−63.9	−60.8	−62.9
τ_2[d]	−57.5	−60.3	−59.1	−60.9	−56.9	−61.0
τ_3[e]	−22.7	48.2	−56.2	50.4	−43.5	43.2
τ_4[f]	−21.9	21.6	24.1	−46.8	47.4	−60.7
β[g]	21.3	15.1	63.2	68.7	61.2	68.0

[a] Distances (Å) and dihedral angles (°) from "level A" calculations (see Exp. Sect.); atomic labels as in Figure 2. [b] Energy differences (kJ·mol^{-1}) are relative to the energy of the respective M*iap* model. [c] N1−C1−C2−N2 dihedral angle. [d] N2−C3−C4−N3. [e] N1−C5−C6−O1. [f] N2−C7−C8−N4. [g] $\beta = \pi/2 - \alpha$, where α is the angle between the M−N_{im} direction and the normal to the imidazole plane (β = 14.8° for La*iap*, ref.[46]).

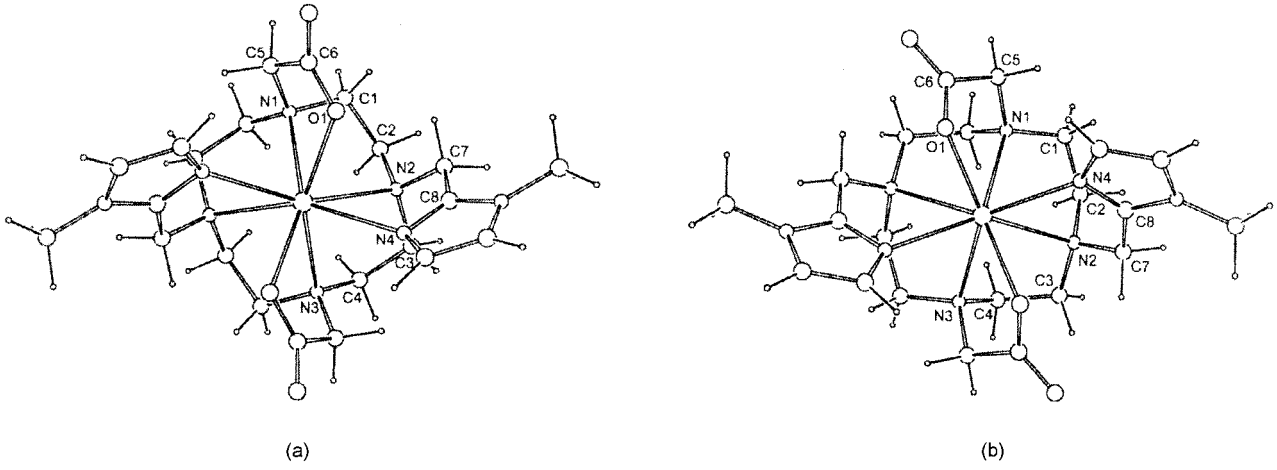

Figure 2. (a) Optimized Cd*iap* conformer geometry, showing the labelling used in Table 1 and in Supporting Information Tables. C_2 symmetry was imposed in the optimizations of all model geometries. (b) Cd*ap* conformer

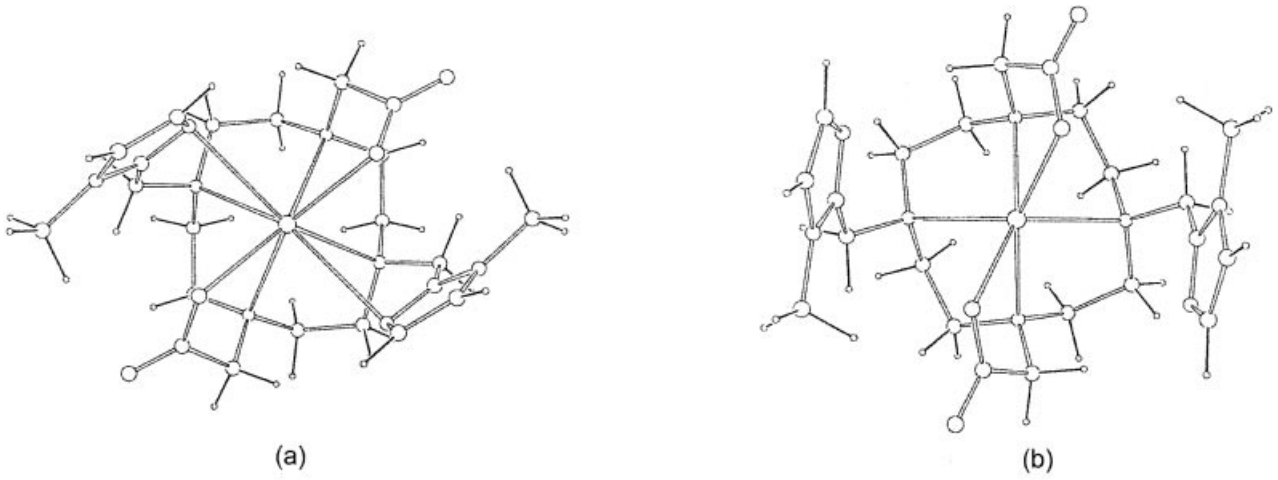

Figure 3. Geometries of the (a) Pb*iap* and (b) Hg*iap* conformers

on the chains by the overall longer metal−donor atom distances in the Pb species − factors that are obviously interrelated to some extent. The Hg conformers are peculiar, as most of their metal−donor distances are significantly shorter than those of Pb (the Hg−N_{mac} and Hg−O bond lengths are close to those of the Cd models), except for the very long Hg−N_{im} interactions (Table 1). The latter distances, which presumably affect the τ_4 values for the Hg models, may be traced to the specific electronic requirements of the Hg^{2+} cation. Indeed, the metal-based part of the HOMO for the Hg conformers has a stereochemically active d-orbital component, whereas the metal contribution to the HOMO of the Pb models has predominantly s (spherical) character; plots of sections of these electron densities are given with the Supporting Information.

Unfortunately, no experimental structure is available for detailed comparison. X-ray structures of Pb complexes formed by pyrazole-functionalized macrocycles revealed appreciable displacements of the metal atom from the planes of coordinating pyrazoles.[42] Previous computational experience with related systems[53] suggests that the overall geometrical features should be reproduced with reasonable accuracy, although individual metal−donor atom distances may be significantly in error. It may be appropriate to note here that the calculations with the SDD metal functions for the Cd systems, referred to in the Exp. Sect., yielded metal−donor atom distances that deviate by 0.012 Å (mean of absolute differences) from those obtained with the LANL2DZ metal functions (Table 1); conversely, for the less tightly bound Pb systems the considerably larger 0.070 Å mean for the absolute difference values was found, the SDD distances being consistently longer than those listed in Table 1. An indirect, but useful, test of the present procedures involves optimizing the geometries of two complex cations that are related to the present compounds and have known structures, namely the Cd[35] and Na[43] derivatives of tetraazacyclododecane functionalized with four pyrazole groups, $[CdL^5]^{2+}$ and $[NaL^5]^{+}$ in the notation of Scheme 3. These optimizations, starting from moderately idealized (C_4 symmetry constraint) but otherwise unbiased geometries [identical (enantiomeric) starting geometries for the two model systems, with parameters borrowed from parts of the present *ap*/*iap* Cd systems], and run at the same level as the present calculations, yielded results in reasonable agreement with experiment (details and graphic representations are shown in the Supporting Information), except for the Cd−N_{mac} distances, which were calculated to be as much as 0.18 Å too long. Such a discrepancy, mostly due to mispositioning of the metal cation between the two planes of donor atoms, was not unexpected for compounds of this type,[53] but should not affect too adversely other geometrical features; in particular, all computed τs are within 2° of the experimental ones. The offset of the metal atom from the heterocycle plane is 0.04 Å for the Cd model (experimental mean value: 0.51 Å) and 0.82 Å for the Na one (experimental, 1.19 Å). Good agreement cannot be expected for the latter quantity, which is very sensitive to the smallest geometrical changes, but the results seem to exclude a computational bias toward bent arrangements of the heterocycle planes, such as those found for the present Pb and Hg models. The increasing metal offset from the heterocycle plane with increasing metal size, from the Cd to the Na test model, found both experimentally and computationally, suggests that the metal−donor distance may be responsible for the predicted arrangements of the Pb and Hg models.

The calculated energy ordering consistently yielded the *iap*-type conformer as slightly more stable than the *ap* one, in agreement with the NMR results. The energy separations (Table 1) indicate that thermally activated interconversion processes between conformers may take place. Although the agreement is gratifying, the definitive assessment of such subtle features is probably beyond these calculations on gas-phase models but, limited to such models, the computed energy orderings may be trusted as merely conformational rearrangements are considered. However, the complexity of such systems may preclude the unequivocal identification of specific factors that determine such energy preferences. In fact a third conformer was found for both the Pb and Hg systems, at slightly higher energy than that of the *ap*-

species. Interestingly, the third conformer is characterized in both cases by shorter $M-N_{im}$ but longer $M-N_{mac}$ distances than the other conformers (details are in the Supporting Information, where the third species is denoted as *ap′* or *iap′*), and features better oriented imidazole groups for coordination to the metal. All four τ signs of these *ap′*/*iap′* species conform to the expected sign distributions for the "pure" *ap* or *iap* types, at variance with results for the lower-energy Pb or Hg conformers (Table 1). Therefore, the attainment of such more regular geometries with these metals seems to involve an energy cost.

As a partial attempt to verify whether solution conditions might affect the arrangement of the dangling groups, reaction field model calculations were undertaken according to Onsager's approach,[54,55] which is based on a spherical solvent cavity and induced-dipole interactions; more explicit treatment of the solvent was difficult due to the size of the systems. Optimizations were performed with a slightly smaller basis than that used for gas-phase calculations (see the Exp. Sect., level B) and were followed by single-point energy calculations at level A. No important changes in geometries were recorded with respect to the vacuum results, and the energy ordering of the conformers was preserved. There were small contractions (< 1%) in the $M-N_{mac}$ and M−O distances and elongations (generally < 2%) of the $M-N_{im}$ distances, except that the loose $M\cdots N_{im}$ interactions of the Hg models (Table 1) decreased by < 1%. The different trends for changes in coordinative bond lengths for the two types of dangling groups might be related to the different overall negative charges localized on them. The torsion angles of the dangling groups were more affected than the metal−donor distances, but with qualitative retention of the arrangements found for the gas-phase models. Parameter values and more details are in Tables S4−S5 of the Supporting Information.

The calculated ^{13}C NMR chemical shifts broadly reproduce the experimental δ values, but are not particularly informative (Table S7). However, the calculated δ's for some carbon atoms of the pendant arms (Table 2), which appear to be sensitive to the *iap* vs. *ap* geometry differences, support the assignment of the *iap* conformer geometry to the species in solution at low temperatures. In particular, there is comparatively better agreement between experimental and calculated δ's for the *iap*-conformer carbon atoms of the acetate arms (those more tightly coordinating), irrespective of the metal atom. The computed δ value for the other arm's methylene carbon moderately favours the *iap* geometry for the Cd derivative, but is inconclusive for both Pb and Hg species. On the one hand, the GIAO calculations do not clarify the arrangement of the imidazole-bearing arms in the Hg complex; on the other hand, they suggest that signals due to those arms' carbon atoms may be insensitive to the geometrical differences predicted between the Hg and the other models.

Table 2. Comparison of computed and experimental ^{13}C NMR shifts[a]

	[CdL^6]			[PbL^6]			[HgL^6]		
	iap	*exp*	*ap*	*iap*	*exp*	*ap*	*iap*	*exp*	*ap*
C6	178.4	177.7	183.8	183.2	178.2	185.3	180.8	176.6	183.4
C5	56.6	57.4	63.1	59.5	54.7	62.9	56.3	56.6	59.7
C7	45.7	48.4	52.6	44.5	49.2	53.8	43.5	47.5	52.9

[a] Shifts (ppm) are calculated from the isotropic shielding tensor value of the Me_4Si carbon (computational level C, see the Exp. Sect.). Atomic labels are as in Figure 2.

Conclusions

Metal−C2 coupling has, perhaps surprisingly, been detected in the NMR spectra of the Cd and Hg derivatives, but not in that of [PbL^6]; however, such discrepancies are not unusual and are not easily rationalized.[7] One might invoke effects of the distinctive HOMO composition of [HgL^6] and/or effects (in the context of a ^3J, rather than ^2J coupling constant) of the shorter $Cd-N_{mac}$ and $Hg-N_{mac}$ distances compared to $Pb-N_{mac}$.

The bonding picture in these compounds set forth by the calculations, featuring two dangling groups less and less strongly bound to the metal, on going from the Cd to the Pb and the Hg derivatives appears to disagree with the similarities in their NMR properties, as well as with the similarities between their NMR behaviour and that of the L^6 lanthanide derivatives,[36] or even of DOTA complexes.[30,38] However, as may be inferred from a previous theoretical investigation,[53] the energetics of the interconversion processes between conformers may not be greatly affected by the presence of two loosely coordinating arms, as long as the other two arms are strongly bound to the metal.

Experimental Section

General Remarks: Commercial solvents were dried from appropriate drying agents just before use according to standard procedures. NMR spectra were obtained with a Varian Gemini g300bb spectrometer, equipped with variable temperature unit, operating at 300 MHz (^1H) and 75.46 MHz (^{13}C). Positive chemical shifts are to high frequency relative to Me_4Si. The variable temperature accessories were checked against methyl alcohol and ethylene glycol. CD_3OH was used as an internal reference for the ^{13}C spectra of the lead derivative. The spectra of the cadmium and mercury derivatives are referred to the CH_3 of the imidazole, whose signal is not affected by the nature of the metal. The $^{13}C\{^1H\}$ NMR spectra of the compounds in the range δ = 55−47 ppm were analyzed with the program CAHOS,[44] which can perform a line-shape fitting by simultaneous refinement of several spectral parameters. Elemental analyses were performed by the Microanalytical Laboratory of the Department of Chemistry of the University of Florence. The ligand H_2L^6 was prepared according to the published procedure.[36] Anhydrous cadmium carbonate (Aldrich), mercuric acetate (Acros) and lead acetate trihydrate (Carlo Erba) were used as received.

Synthesis of [CdL^6]·3H$_2$O: Neat $CdCO_3$ (43 mg, 0.25 mmol) was added to a solution of the ligand $H_2L^6\cdot 2H_2O$ (128 mg, 0.25 mmol) in H_2O (15 cm^3) and the resulting suspension warmed (ca. 60 °C) for 2 h; the remaining solid was eliminated by centrifugation and

the solvent was removed in a desiccator under vacuum at room temperature. The resultant complex was recrystallized from CH_3CN and toluene; yield 65%. ^1H NMR (D_2O, 273 K, C_M = $9.2\cdot10^{-2}$, pD = 7.3): δ = 6.69 (d, J = 1.2 Hz, 2 H, H imidazole), 6.42 (d, J = 1.2 Hz, 2 H, H imidazole), 3.69 (d, J = 15.4 Hz, 2 H, CH_2 acetate), 3.34 (d, J = 15.3 Hz, 2 H, CH_2 acetate), 3.28 (s, 6 H, CH_3 imidazole), 3.01 (t, J = 11.9 Hz, 2 H, CH_2 macrocycle), 2.91 (t, J = 12.0 Hz, 2 H, CH_2 macrocycle), 2.67 (t, J = 12.5 Hz, 2 H, CH_2 macrocycle), 2.56 (d, J = 16.5 Hz, 2 H, CH_2 imidazole), 2.37 (t, J = 12.8 Hz, 2 H, CH_2 macrocycle), 2.28 (m, 6 H, CH_2 imidazole and CH_2 macrocycle), 2.05 (d, J = 12.9 Hz, 2 H, CH_2 macrocycle) and 1.86 (d, J = 12.9 Hz, 2 H, CH_2 macrocycle) ppm. $^{13}C\{^1H\}$ NMR: δ = 177.7 (COO^-), 145.8 (d, $^2J^{13}_{C\text{-}^{111}Cd}$ = 13.1 Hz, C^2 imidazole), 125.6, 122.5 (C^4, C^5 imidazole), 57.4 (CH_2COO^-), 51.8, 50.9, 48.4, 48.1 (CH_2 macrocycle), 48.4 (CH_2 imidazole) and 32.0 (CH_3 imidazole) ppm. $C_{22}H_{40}CdN_8O_7$ (641.0): calcd. C 41.2, H 6.3, N 17.5; found C 40.9, H 6.3, N 17.3.

Synthesis of $[ML^6]\cdot3H_2O$ (M = Hg, Pb): $Hg(CH_3COO)_2$ (0.25 mmol) dissolved in water (5 cm^3) was added to $H_2L^6\cdot2H_2O$ (0.25 mmol) in water (8 cm^3); the solution was then gently warmed (ca. 40 °C) for 5 h. After cooling, the pH was adjusted to 7.3 by adding Na_2CO_3 dissolved in water. The solvent was then removed at room temperature in a desiccator under vacuum and the obtained solid was recrystallized from CH_3CN and toluene; yield 60%. The lead derivative was obtained by the same procedure by adding $Pb(CH_3COO)_2\cdot3H_2O$ dissolved in water to a water solution of the ligand; yield 65%. $C_{22}H_{40}HgN_8O_7$ (729.2): calcd. C 36.2, H 5.5, N 15.4; found C 36.4, H 5.4; N. 14.6. ^1H NMR (D_2O, 273 K, c_M = $8.5\cdot10^{-2}$, pD = 7.3): δ = 6.76 (d, J = 1.3 Hz, 2 H, H imidazole), 6.44 (d, J = 1.2 Hz, 2 H, H imidazole), 3.73 (d, J = 15.6 Hz, 2 H, CH_2 acetate), 3.45 (d, J = 15.6 Hz, 2 H, CH_2 acetate), 3.29 (s, 6 H, CH_3 imidazole), 2.85 (m, 6 H, CH_2 macrocycle), 2.40 (m, 10 H, CH_2 imidazole and CH_2 macrocycle), 2.10 (d, J = 12.6 Hz, 2 H, CH_2 macrocycle) and 1.90 (d, J = 12.6 Hz, 2 H, CH_2 macrocycle) ppm. $^{13}C\{^1H\}$ NMR (D_2O, 273 K, c_M = $8.5\cdot10^{-2}$, pD = 7.3): δ = 176.6 (COO^-), 145.1 (d, $^2J^{13}_{C\text{-}^{199}Hg}$ = 54.5 Hz, C^2 imidazole), 125.6, 122.7 (C^4, C^5 imidazole), 56.6 (CH_2COO^-), 50.9, 50.6, 48.3, 47.5 (CH_2 macrocycle), 47.5 (CH_2 imidazole) and 32.0 (CH_3 imidazole) ppm.

$C_{22}H_{40}N_8O_7Pb$ (735.8): calcd. C 35.9, H 5.5, N 15.2; found C 36.0, H 5.4; N. 15.0. ^1H (D_2O, 273 K, c_M = $8.8\cdot10^{-2}$, pD = 7.2): δ = 6.74 (d, J = 1.3 Hz, 2 H, H imidazole), 6.50 (d, J = 1.3 Hz, 2 H, H imidazole), 3.98 (d, J = 15.6 Hz, 2 H, CH_2 acetate), 3.82 (d, J = 15.8 Hz, 2 H, CH_2 acetate), 3.27 (s, 6 H, CH_3 imidazole), 3.07 (m, 10 H, CH_2 macrocycle), 2.74 (t, J = 13.0 Hz, 2 H, CH_2 macrocycle), 2.48 (m, 6 H, CH_2 imidazole and CH_2 macrocycle) and 2.34 (d, J = 12.0 Hz, 2 H, CH_2 macrocycle) ppm. $^{13}C\{^1H\}$ (D_2O, 273 K, c_M = $8.8\cdot10^{-2}$, pD = 7.2): δ = 178.2 (COO^-), 145.4 (C^2 imidazole), 124.4, 123.1 (C^4, C^5 imidazole), 57.4 (CH_2COO^-), 53.3, 52.3, 49.9, 49.4 (CH_2 macrocycle), 49.2 (CH_2 imidazole) and 32.1 (CH_3 imidazole) ppm.

Computational Procedures: Calculations on the neutral $[ML^6]$ model systems (M = Cd, Pb, Hg) were performed with the GAUSSIAN 98 suite of programs,[45] generally using the hybrid HF-DFT B3LYP method.[46–48] Unless specified differently, the 6-311G(d) basis set was used for all non-metal atoms.[45,49] For the Cd and Pb atoms the LANL2DZ valence and effective core potential functions,[50] as well as their SDD counterparts,[51,52] were used for comparison purposes (only results from the former set of calculations are reported in some detail). For Hg the SDD functions were initially used and the lengthy calculations were not repeated with the alternative functions as no detailed comparisons were sought between systems formed with the different metal atoms. For brevity, the computational level B3LYP/6−311G(d) with LANL2DZ (Cd, Pb) or SDD (Hg) functions will be referred to as "level A". Geometry optimizations on gas phase models were performed with the C_2 symmetry restraint, all atoms being included. Initial geometries were from the previously investigated lanthanide analogs[53] or were applied by cross assignments, e.g. starting a Pb-model optimization from an optimized Hg-model geometry, and so on. The nature of stationary points as true minima was checked by frequency calculations, and unscaled ZPE corrections were applied to the energy values. To mimic conditions in solution, calculations (without vibrational analysis) were undertaken according to Onsager's reaction field (SCRF) approach,[54,55] at the B3LYP/6-311G(d)//B3LYP/6-31G(d) level (level B), with the above LANL2DZ/SDD metal functions. NMR shielding tensors were obtained by GIAO[56] [HF/6-311G(d) calculations on the vacuum-optimized geometries computational level C: HF/6-311G(d)//B3LYP/6-311G(d), with metal functions as above], chemical shifts for carbon atoms being calculated with respect to the 194.51 isotropic shielding tensor obtained for the Me_4Si carbon, at the same level C. For graphics, Molden[57] and ORTEP[58,59] were employed.

Acknowledgments

We acknowledge financial support by the Italian Ministero dell'Istruzione, dell'Università e della Ricerca.

[1] L. F. Lindoy, in *The Chemistry of Macrocyclic Ligand Complexes*, Cambridge University Press, Cambridge, **1989**.
[2] R. D. Hancock, A. E. Martell, *Chem. Rev.* **1989**, *89*, 1875−1914.
[3] P. V. Bernhardt, G. A. Lawrance, *Coord. Chem. Rev.* **1990**, *104*, 297−343.
[4] D. Parker, K. Pulukkody, T. J. Norman, A. Harrison, L. Royle, C. Walker, *J. Chem. Soc., Chem. Commun.* **1992**, 1441−1443.
[5] R. Dhillon, A. K. W. Stephens, S. L. Whitbread, S. F. Lincoln, K. P. Wainwright, *J. Chem. Soc., Chem. Commun.* **1995**, 97−98.
[6] D. Parker, J. A. G. Williams, *J. Chem. Soc., Dalton Trans.* **1996**, 3613−3628.
[7] H. Maumela, R. D. Hancock, L. Carlton, J. H. Reibenspies, K. P. Wainwright, *J. Am. Chem. Soc.* **1995**, *117*, 6698−6707.
[8] M. Di Vaira, F. Mani, N. Nardi, P. Stoppioni, A. Vacca, *J. Chem. Soc., Dalton Trans.* **1996**, 2679−2684.
[9] M. Di Vaira, F. Mani, P. Stoppioni, *J. Chem. Soc., Dalton Trans.* **1998**, 1879−1884.
[10] R. Dhillon, S. F. Lincoln, S. Madbak, A. K. W. Stephens, K. P. Wainwright, S. L. Whitbread, *Inorg. Chem.* **2000**, *39*, 1855−1858.
[11] M. G. B. Drew, *Coord. Chem. Rev.* **1977**, *24*, 179−275.
[12] I. Murase, I. Ueda, N. Marubayashi, S. Kida, N. Matsumoto, M. Kudo, M. Toyohara, K. Hiate, M. Mikuriya, *J. Chem. Soc., Dalton Trans.* **1990**, 2763−2769.
[13] L. H. Tan, M. R. Taylor, K. P. Wainwright, P. A. Duckworth, *J. Chem. Soc., Dalton Trans.* **1993**, 2921−2928.
[14] K. P. Wainwright, *Adv. Inorg. Chem.* **2001**, *52*, 293−334.
[15] V. Balzani, J. M. Lehn, J. Van de Loosdrecht, A. Mecati, N. Sabbatini, R. Ziessel, *Angew. Chem. Int. Ed. Engl.* **1991**, *30*, 190−191.
[16] D. Parker, J. A. G. Williams, *Chem. Commun.* **1998**, 245−246.
[17] D. Parker, *Chem. Br.,* 1994, **30**, 818−822.
[18] *Comprehensive Supramolecular Chemistry* (Eds.: J.-M. Lehn, D. D. Macnicol, J. L. Atwood, J. E. Davies, D. N. Reinhoudt, F. Vogtle), Pergamon: Oxford, 1996; Vol. 10, ch. 17.
[19] B. Barbier, A. Brack, *J. Am. Chem. Soc.* **1988**, *110*, 6880−6882.
[20] Y. Matsumoto, M. Komiyama, *J. Chem. Soc., Chem. Commun.* **1990**, 1050−1051.

[21] K. O. A. Chin, J. R. Morrow, *Inorg. Chem.* **1994**, *33*, 5036−5041.
[22] L. Carlton, R. D. Hancock, H. Maumela, K. P. Wainwright, *J. Chem. Soc., Chem. Commun.* **1994**, 1007−1008.
[23] S. Buøen, J. Dale, P. Groth, J. Krane, *J. Chem. Soc., Chem. Commun.* **1982**, 1172−1174.
[24] C. M. Madeyski, J. P. Michael, R. D. Hancock, *Inorg. Chem.* **1984**, *23*, 1487−1489.
[25] A. K. W. Stephens, S. F. Lincoln, *J. Chem. Soc., Dalton Trans.* **1993**, 2123−2126.
[26] K. O. A. Chin, J. R. Morrow, C. H. Lake, M. R. Churchill, *Inorg. Chem.* **1994**, *33*, 656−664.
[27] M. R. Spirlet, J. Rebizant, J. F. Desreux, M. F. Loncin, *Inorg. Chem.* **1984**, *23*, 359−363.
[28] J. P. Dubost, J. M. Leger, M. H. Langlois, D. Meyer, M. Schaefer, *C. R. Acad. Sci. Paris, Ser. II* **1991**, *312*, 349−354.
[29] S. Aime, A. Barge, M. Botta, M. Fasano, J. D. Ayala, G. Bombieri, *Inorg. Chim. Acta* **1996**, *246*, 423−429.
[30] S. Aime, A. Barge, F. Benetollo, G. Bombieri, M. Botta, F. Uggeri, *Inorg. Chem.* **1997**, *36*, 4287−4289.
[31] J. R. Morrow, S. Amin, C. H. Lake, M. R. Churchill, *Inorg. Chem.* **1993**, *32*, 4566−4572.
[32] S. Aime, A. S. Batsanov, M. Botta, J. A. K. Howard, D. Parker, K. Senanayake, G. Williams, *Inorg. Chem.* **1994**, *33*, 4696−4706.
[33] M. Di Vaira, F. Mani, P. Stoppioni, *J. Chem. Soc., Chem. Commun.* **1989**, 126−127.
[34] M. Di Vaira, F. Mani, P. Stoppioni, *J. Chem. Soc., Dalton Trans.* **1992**, 1127−1130.
[35] M. Di Vaira, F. Mani, M. Menicatti, R. Morassi, P. Stoppioni, *Polyhedron* **1997**, *16*, 3585−3591.
[36] F. Mani, R. Morassi, P. Stoppioni, A. Vacca, *J. Chem. Soc., Dalton Trans.* **2001**, 2116−2120.
[37] E. Tóth, E. Brucher, I. Lázár, I. Tóth, *Inorg. Chem.* **1994**, *33*, 4070−4076.
[38] J. F. Desreux, *Inorg. Chem.* **1980**, *19*, 1319−1324.
[39] S. Aime, M. Botta, G. Ermondi, *Inorg. Chem.* **1992**, *31*, 4291−4299.
[40] S. Aime, M. Botta, M. Fasano, M. P. M. Marques, C. F. G. C. Geraldes, D. Pubanz, A. E. Merbach, *Inorg. Chem.* **1997**, *36*, 2059−2068.
[41] A. K. W. Stephens, R. S. Dhillon, S. E. Madbak, S. L. Whitbread, S. F. Lincoln, *Inorg. Chem.* **1996**, *35*, 2019−2024.
[42] M. Di Vaira, M. Guerra, F. Mani, P. Stoppioni, *J. Chem. Soc., Dalton Trans.* **1996**, 1173−1179.
[43] G. de Martino Norante, M. Di Vaira, F. Mani, S. Mazzi, P. Stoppioni, *J. Chem. Soc., Chem. Commun.* **1990**, 438−439.
[44] F. Cecconi, C. A. Ghilardi, P. Innocenti, S. Midollini, A. Orlandini, A. Ienco, A. Vacca, *J. Chem. Soc., Dalton Trans.* **1996**, 2821−2826.
[45] Frisch, M. J., G. W. Trucks, H. B. Schlegel, G. E. Scuseria, M. A. Robb, J. R. Cheeseman, V. G. Zakrzewski, J. A. Montgomery, Jr., R. E. Stratmann, J. C. Burant, S. Dapprich, J. M. Millam, A. D. Daniels, K. N. Kudin, M. C. Strain, O. Farkas, J. Tomasi, V. Barone, M. Cossi, R. Cammi, B. Mennucci, C. Pomelli, C. Adamo, S. Clifford, J. Ochterski, G. A. Petersson, P. Y. Ayala, Q. Cui, K. Morokuma, D. K. Malick, A. D. Rabuck, K. Raghavachari, J. B. Foresman, J. Cioslowski, J. V. Ortiz, A. G. Baboul, B. B. Stefanov, G. Liu, A. Liashenko, P. Piskorz, I. Komaromi, R. Gomperts, R. L. Martin, D. J. Fox, T. Keith, M. A. Al-Laham, C. Y. Peng, A. Nanayakkara, C. Gonzalez, M. Challacombe, P. M. W. Gill, B. Johnson, W. Chen, M. W. Wong, J. L. Andres, C. Gonzalez, M. Head-Gordon, E. S. Replogle, J. A. Pople, Gaussian 98, Revision A.7, Gaussian, Inc., Pittsburgh PA (USA), **1998**.
[46] A. D. Becke, *J. Chem. Phys.* **1993**, *98*, 5648−5652.
[47] A. D. Becke, *J. Chem. Phys.* **1993**, *98*, 1372−1377.
[48] C. Lee, W. Yang, R. G. Parr, *Phys. Rev. B: Condens. Matter Mater. Phys.* **1988**, *37*, 785−789.
[49] R. Krishnan, J. S. Binkley, R. Seeger, J. A. Pople, *J. Chem. Phys.* **1980**, *72*, 650−654.
[50] P. J. Hay, W. R. Wadt, *J. Chem. Phys.* **1985**, *82*, 270−283.
[51] M. Dolg, H. Stoll, A. Savin, H. Preuss, *Theor. Chim. Acta* **1989**, *75*, 173−194.
[52] A. Bergner, M. Dolg, W. Kuechle, H. Stoll, H. Preuss, *Mol. Phys.* **1993**, *80*, 1431−1441.
[53] M. Di Vaira, P. Stoppioni, *New J. Chem.* **2002**, *26*, 136−144.
[54] L. Onsager, *J. Am. Chem. Soc.* **1936**, *58*, 1486−1493.
[55] M. W. Wong, K. B. Wiberg, M. J. Frisch, *J. Am. Chem. Soc.* **1992**, *114*, 1645−1652.
[56] K. Wolinski, J. F. Hinton, P. Pulay, *J. Am. Chem. Soc.* **1990**, *112*, 8251−8260.
[57] G. Schaftenaar, J. H. Noordik, *J. Comput.-Aided Mol. Design* **2000**, *14*, 123−134.
[58] C. K. Johnson, *ORTEP*, Report ORNL-5138, Oak Ridge National Laboratory, Oak Ridge, TN, USA, **1976**.
[59] L. J. Farrugia, *J. Appl. Crystallogr.* **1997**, *30*, 565.

Received March 31, 2003

